Journal of Visualization, Vol. 10, No. 2 (2007)207-215

Regular Paper

Measurement of Particle Distribution in Microchannel Flow Using a 3D-TIRFM Technique

Kanda, K.*[1], Ogata, S.,*[2] Jingu, K.*[2] and Yang, M.*[2]

*1 Advanced Software Technology & Mechatronics Research Institute, Creation Core Kyoto Mikuruma 310, 448-5 Kajiicho, Kamigyo-ku, Kyoto 602-0841, Japan. E-mail: kanda@astem.or.jp
*2 Graduate School of Engineering, Tokyo Metropolitan University, 1-1 Minamiohsawa, Hachiohji-shi, Tokyo 192-0397, Japan.

Received 18 May 2006
Revised 28 September 2006

Abstract : The presence of bio-substances in the near-wall region in micro bio-chemical analysis chips is an important topic but one which is difficult to investigate directly. In this paper we developed an accurate 3D-TIRFM technique, which was used to investigate the three-dimensional positions of nano-particles. The depth was calibrated using a piezo stage. As an example of an application of this technique, the concentration profile of nano-particles near a wall surface was investigated. The results showed that the concentration profile was non-uniform and lower than that in the bulk. In addition the ionic strength of the solvent strongly influenced the concentration profile. It was concluded that the non-uniform concentration profile is due to the influence of the electric double layer around the particles and the surface. This demonstrates the importance of selecting suitable electric characteristics, since a non-uniform and low concentration profile near the wall will affect the reaction efficiency and the sensitivity in micro bio-chemical analysis.

Keywords : Evanescent light, Microchannel flow, Concentration profile, Near wall, 3D-TIRFM.

1. Introduction

Over the past two decades micro bio-chemical chips, often referred to as micro Total Analysis Systems (μTAS) or Lab on Chips (LOC), have attracted a considerable amount of attention due to the fact that miniaturization of reaction systems results in shorter reaction times, reduces the required amount of sample and reagent and improves the controllability of the reaction temperature. The shorter reaction time is a result of the increase in the ratio of the diffusion length of the substance to the characteristic length of the reaction region upon miniaturization (Sato et al., 2003).

There have been a large number of studies done that have investigated the advantages of microchips (e.g., Uchiyama et al., 2004). In particular, micro immune-assay chips, in which bio-substances generate immune reactions on the surface of beads or walls in a micro channel, have attracted a considerable amount of attention (e.g., Do and Ahn, 2005 and Bernard et al, 2001) because they take advantage of the increased surface-to-volume ratio. Bio-substances flow in micro channels as they approach a wall by self-diffusion and they interact with the wall surface, which is chemically modified. However, there are a variety of wall effects, such as physicochemical DLVO forces (Israelachivili, 1991) and hydrodynamic shear lift (Feng et al., 1994) that occur near the wall surface. As a consequence of these wall effects, reducing the characteristic length does not always ensure that reactions become more rapid. Although there have been many studies that have achieved

miniaturization of bio-chemical reactions using micro bio-chemical chips, these surface effects have not been taken into account for conventional micro-biochemical chips. However, it is difficult to estimate the surface effect for bio-substances because of their complexity. Dynamic observation of the bio-substances near a wall is essential for analyzing surface effects. Gaining an understanding of near-wall phenomena can improve reaction times in microchips that utilize reactions on the wall surface.

Evanescent light wave is a useful light source for illuminating the near-wall region, where the wall effects take place. Figure 1 shows a conceptual diagram of the evanescent light wave generated by total internal reflection. As the angle of incidence of the light incident on an interface with a medium having a different refractive index increases, it reaches a critical angle $\theta_c = \sin^{-1}(n_2/n_1)$. At angles greater than the critical angle, the light is completely reflected at the interface, i.e., total internal reflection occurs. On a micro-level, however, a portion of the incident light penetrates the interface, enters the external medium and propagates parallel to the surface in the plane of incidence, creating a surface wave. The intensity of the evanescent wave decays exponentially with the distance z from the two-medium interface,

$$I(z) = I_0 \exp(-z/\delta) \tag{1}$$

where I_0 is the light intensity at the interface and δ is the evanescent wave penetration depth. The penetration depth, which characterizes the evanescent field, can be calculated as:

$$\delta = (\lambda_0/4\pi)(n_1^2 \sin^2\theta - n_2^2)^{1/2} \tag{2}$$

where λ_0 is the wavelength of the incident light and θ is the incident angle. The penetration depth is typically smaller than λ_0.

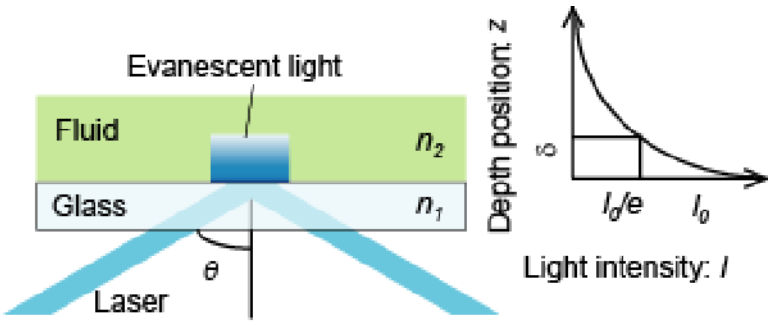

Fig. 1. Conceptual diagram of an evanescent light wave generated by total internal reflection.

Total internal reflection fluorescent microscopy (TIRFM), which combines evanescent light waves and fluorescence for observing near-wall phenomena, is frequently used in the fields of surface science and fluid engineering. Jin et al. (2004) applied this technique to investigate the slip boundary conditions of microchannel flow near a hydrophobic wall. They successively measured the mean flow velocity inside the region illuminated by the evanescent light wave using particle imaging velocimetry (PIV). However, they were not able to obtain depth information, but instead measured an averaged velocity. Zettner and Yoda (2003) and Sadr et al. (2004) developed nano-particle image velocimetry using TIRFM for near-wall velocimetry. Furthermore, Kihm et al. (2004) proposed a method for determining three-dimensional (3D) particle position using TIRFM and used it to investigate the Brownian motion of particles in the near-wall region. They acquired depth information of the particle ratiometrically, based on the exponential decay of the intensity of the evanescent wave with depth (see Eq. (1)). They determined the wall position by measuring the intensity of the particle attached to the wall surface. Therefore, experimental parameters such as the penetration depth δ and the reference intensity I_0 are critical parameters for determining the uncertainty of the measurement. In addition, it is difficult ascertain the absolute particle position. Sadr et al. (2005) performed an accurate analysis of the effects of hindered Brownian motion on nano-particle image velocimetry. They used particles that were 100-1000 nm in diameter and concluded that the errors due to Brownian diffusion-induced particle mismatch are negligible

compared with other sources of experimental error.

To achieve more accurate measurement of the 3D particle positions near a wall, it is necessary to calibrate the depth of the particle. In this study, we developed a 3D-TIRFM technique for micro bio-chemical chips, based on the technique developed by Kihm et al. (2004), and calibrated particle depth using a piezo stage.

2. Experimental Procedures

2.1 3D-TIRFM Technique

For micro bio-chemical applications, the particle size should be small because bio-substances used in chips are usually very small. Jin et al. (2004) and Kihm et al. (2004) employed fluorescent particles having sub-micron diameters (200 nm and 300 nm, respectively). We used particles having a 100-nm diameter (505 nm/515 nm yellow-green fluorescent, Molecular Probe Inc., F8803, carboxylate modified) as the quasi bio-substance. Figure 2 shows a schematic illustration of the experimental setup which is based on an objective-lens-based TIRFM system using an Olympus Plan APO 60x oil-immersion TIRF objective lens having a numerical aperture of 1.45. The experimental setup consists of an inverted microscope (Olympus Inc., IX-71), a continuous-wave (CW) Ar-ion laser having an output wavelength of 488 nm (Melles Griot, IMA-100) and an intensified charge-coupled device (CCD) camera (Hamamatsu Co., C5909). The solution containing the fluorescent particles was introduced into a polydimethylsiloxane (PDMS)-glass microchannel located on the microscope stage by a syringe pump (Harvard Apparatus, PHD-2000). The beam from the Ar-ion laser irradiated the glass-fluid interface at the critical angle, which was 60.7° for this system. The totally reflected light generated evanescent light, which illuminated the region near the interface and excited the fluorescent particles in the fluid. Fluorescent-light images of the particles were captured using an intensified CCD camera. The nanoparticles had a specific gravity of 1.05 and carry weak negative charges because of their COOH- group. The variation in the particle sizes was less than ±2.5 %. A PDMS-glass microchannel chip was fabricated by photolithography and a molding technique. Figure 3 shows a diagram illustrating the process. SU-8 (Micro Chem Co., SU-8 3000) was deposited on a glass plate as the channel template by a general photolithography process. Then PDMS was molded onto the template and dried in a dry oven at 60˚C for one hour. The PDMS microchannel was peeled from the template and was bonded to a cover slip by heating in a dry oven at 120˚C for four hours. The microchannel was 50 μm deep, 1 mm wide and 10 mm long.

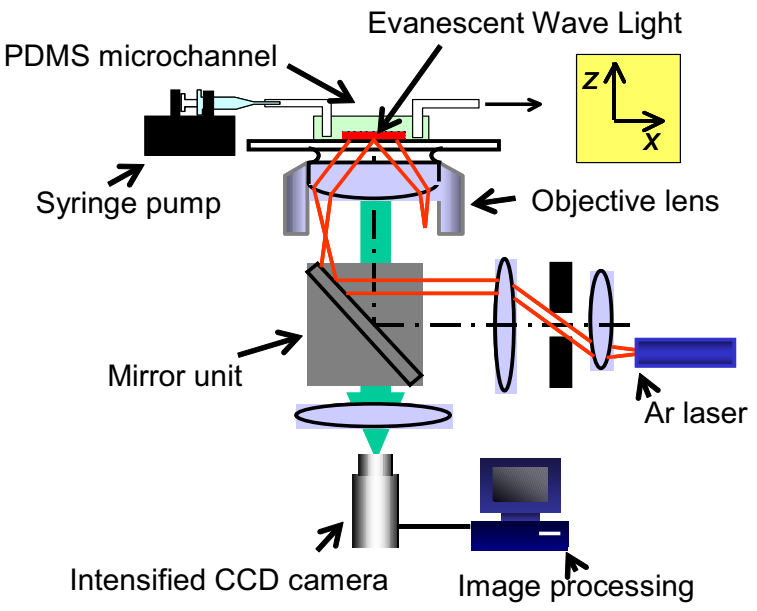

Fig. 2. Experimental system for generating evanescent light inside a PDMS microchannel.

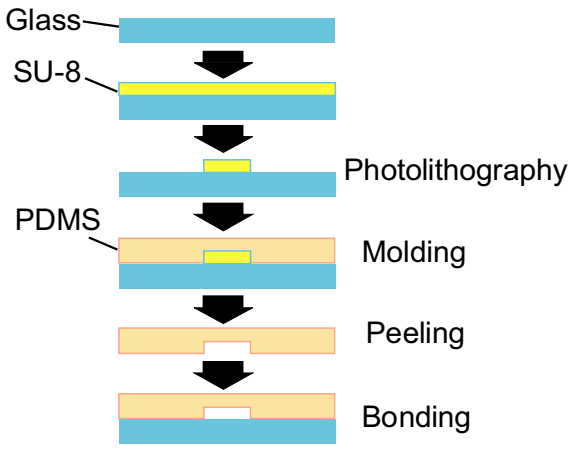

Fig. 3. Processing steps for producing a PDMS microchip.

Figure 4 shows a typical particle image obtained using the system. Figure 4(a) shows the fluorescent particles illuminated by the radiation from the laser which penetrates the channel. The fluorescent particles in Fig. 4(b) are illuminated by evanescent light when the incident angle is 61.9˚. The images of the particles in Fig. 4(b) are distinct, while those in Fig. 4(a) are indistinct making it is difficult to distinguish individual particles. Each bright spot in Fig. 4(b) represents an individual particle and the individual particles clearly have a range of intensities. The fluorescent light intensity is determined by the evanescent light intensity at the particle depth. Therefore the depth of the particle can be estimated from the evanescent light intensity, given in Eq. (1). The two-dimensional particle position was taken to be the center of the particle's image because the particle intensity profiles generally have a Gaussian profile. In the PIV technique, particle images in a pair of images are cross-correlated and the particle velocities are measured in general. The measurement error is estimated from the optical "particle visibility", defined as the ratio of the peak intensity of the particle image when it is in focus to the background intensity (Olsen and Adrian, 2000) and from the Brownian diffusion of tracer particles. It is necessary to take the error into account when measuring the velocity field. In this paper, the 3D-positional errors are principally discussed since it is desired to measure the distribution of the particles. The influence of out-of-plane particles is negligible for the nano-PIV technique since the evanescent illumination does not extend beyond the focal plane. Other experimental errors are described in Section 4.

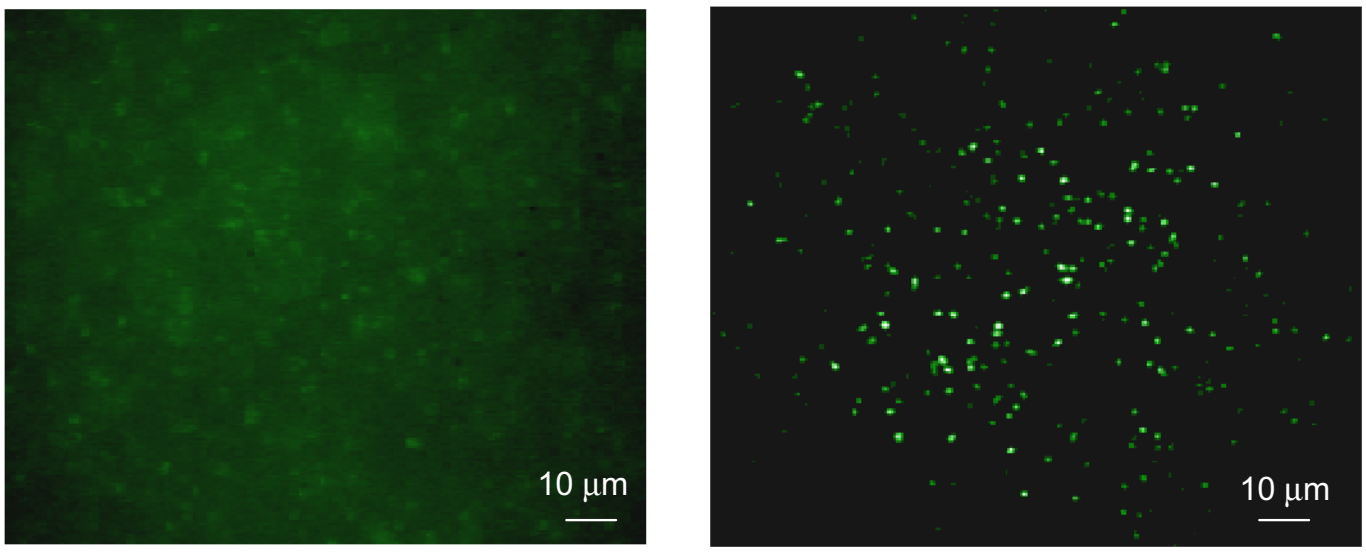

(a) Laser illumination penetrating the channel (at an incident angle smaller than the critical angle).

(b) Evanescent light illumination (incident angle = 61.9˚, average number of particles in a frame is 512).

Fig. 4. Comparison of images obtained with (a) normal laser light illumination and (b) evanescent light illumination (640 x 480 pixels).

2.2 Calibration of Particle Depth

The measured depths for conventional TIRFM technique generally include an uncertainty derived from errors such as the reference intensity of the particle (the wall position), the incident angle of the laser light and the standard depth (the penetration depth of the evanescent light). Direct calibration of the particle position is problematic because it is difficult to measure the particle position to nano-scale accuracy in an extremely small system by another method. In this paper, direct calibration of the particle depth using a piezo stage was attempted and the uncertainty was calculated. The relationship between the particle depth and the fluorescent intensity of the particle was experimentally measured using the experimental system shown in Fig. 5. A pin was fixed on a piezo stage (Jena GmbH, piezo system TRIOR 100 CAP). A stainless-steel sphere having a 2-mm diameter was bonded to one side of the pin using epoxy resin. Fluorescent particles were absorbed on the ball surface by immersing it for 10 min in a suspension of fluorescence particles in water. For the calibration we used the image of a single particle absorbed on the ball and ensured that the particles were not aggregated.

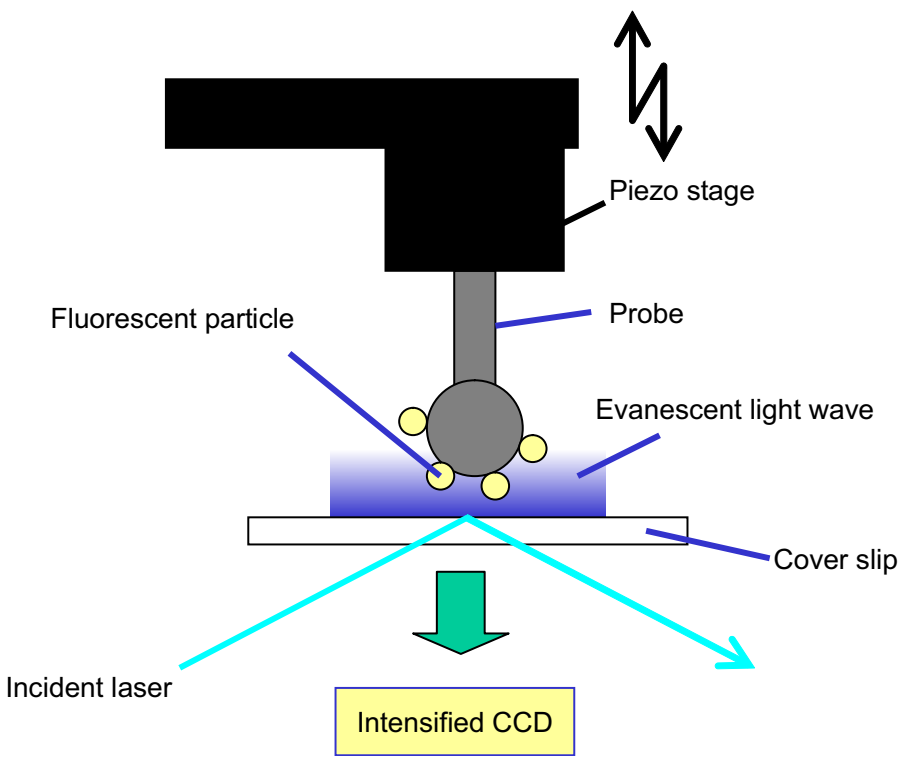

Fig. 5. Experimental setup for calibrating the depth of particles.

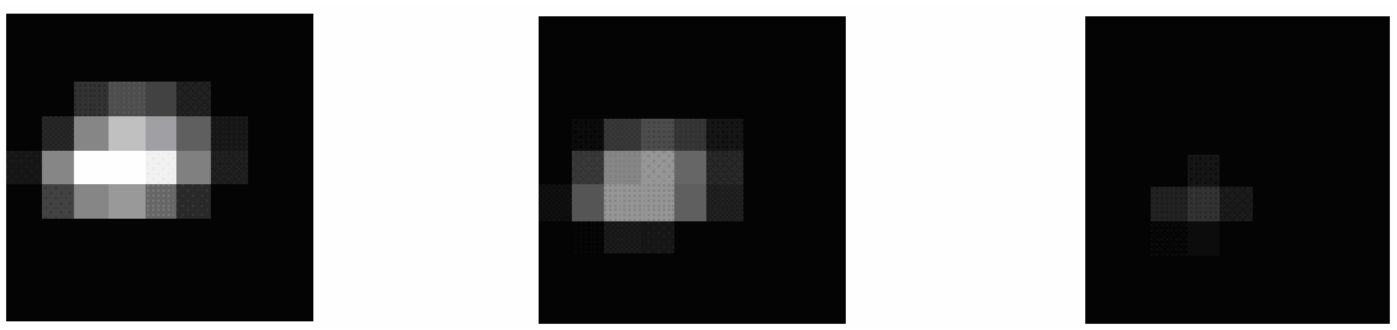

(a) z = 0 nm (b) z = 80 nm (c) z = 200 nm

Fig. 6. Typical particle images obtained at different depths.

A cover slip was placed on the microscope stage and distilled water was dropped onto it. The light from the Ar-ion laser was used to generate evanescent light at the interface. The ball was lowered into the distilled water using the piezo stage and images of the particle were recorded using the intensified CCD camera. The CCD gain was adjusted so that saturation did not occur. Typical particle images are shown in Fig. 6. From this figure it can be seen that the fluorescent intensity of the particle decreases as the particle's distance from the interface increases. At the wall position (z = 0), the intensity of the fluorescent particle does not vary even if the probe is brought closer to the interface. The relationship between the particle's depth and the fluorescent intensity of the particle is shown in Fig. 7. The light intensity of the fluorescent particle decays exponentially and it depends on the penetration depth of the evanescent light. The curves of fluorescent light intensity were fitted using Eq. (1) and normalized. Specifically, the depth δ was determined from the experimental data shown in Fig. 7 by means of the least mean square method. The relationship between the fluorescent light intensity I' and the particle's depth z is then expressed as:

$$z = -k\delta \log(I_0' / I'(z)) \tag{3}$$

where I_0' is the fluorescent light intensity of the particle at the interface and k is the calibration coefficient (= 0.55 in our measurements). In this calibration, k = 0.55 was derived by fitting the penetration depth, since the measurements were conducted at several penetration depths. This figure is valid for measurements in which the penetration depth lies within the range 193 to 306 nm

(see Fig. 7). Equation (3) is based on the assumption that the light intensity of the fluorescent particle decays exponentially with depth. The depth directional position-error estimated from the variation between Eq. (3) and the results shown in Fig. 7 was 9.1 %. Note that the depth of the particle z refers to the distance between the wall surface and the bottom point of the particle. The maximum resolution for the depth of the particle is shown in Fig. 8. The maximum resolution shown in Fig. 8 is the extent of depth per unit intensity signal. The resolution increases as the particle approaches the surface of the interface.

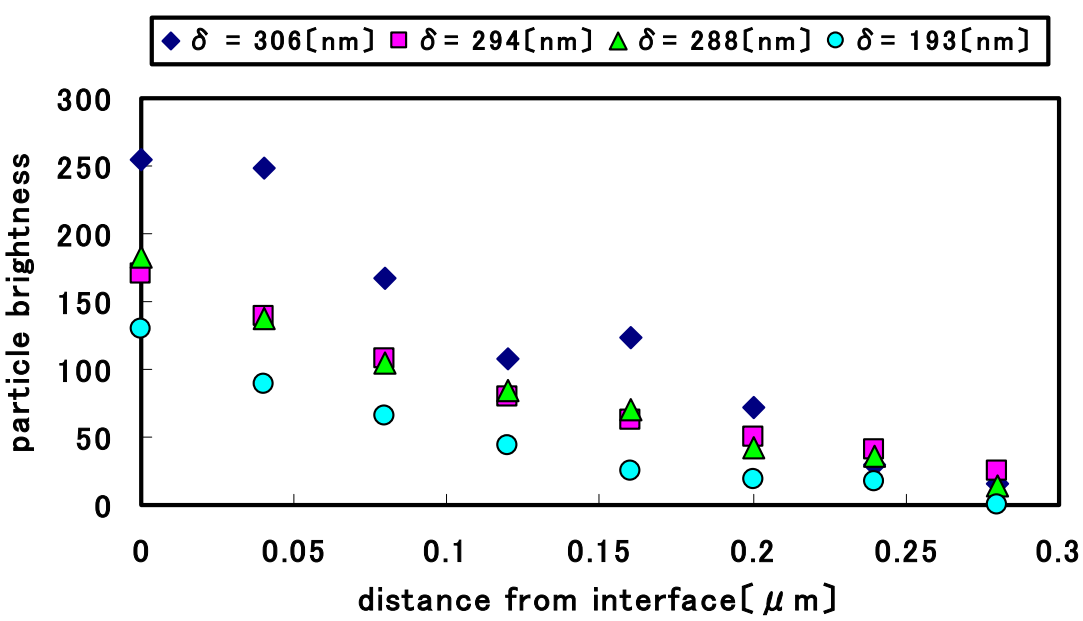

Fig. 7. Relationship between the particle depth and the particle intensity.

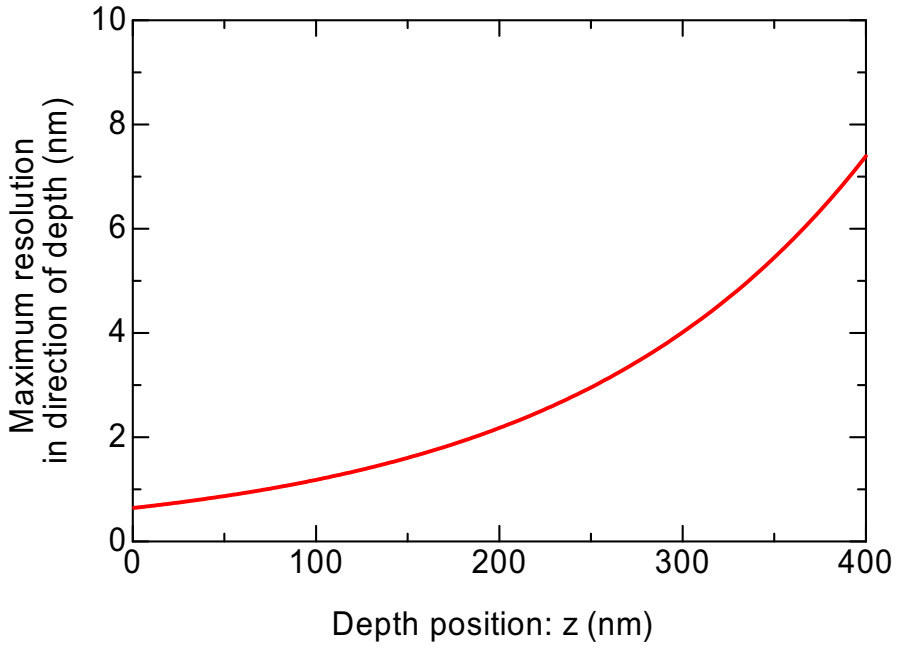

Fig. 8. Maximum resolutions as a function of depth.

3. Measurement of the Near-Wall Concentration Profile of Particles

For microchip analysis utilizing reactions on the surface, such as surface plasmon resonance or fluorescent detection, it is important to determine the 3D concentration profile of the bio-substance. The concentration profile of nano-particles in the near-wall region was measured in order to evaluate the surface effect using the TIRFM technique proposed in this study. The measurement of concentration profile is valuable for investigating the behavior of bio-substances and the influence of

the surface. Fluorescent particles having a diameter of 100 nm were employed as the quasi-bio-substance in the same manner as in Section 2.

Two solutions of different ionic strengths, distilled water (pH 5.6) and a phosphate buffer solution (pH 7.0, 0.001 M) were employed. The fluorescent particles were suspended in the solutions at a volume concentration of 10^{-3} %. The channel surface (-SiOH) and the fluorescent particles (-COOH) have electrical charge in an electrolyte solution. Charged surfaces have an electric double layer in the vicinity of their surfaces. It is expected that solutions having higher ionic strengths have thinner electric double layers (i.e., shorter Debye lengths) and larger surface potentials (Israelachivili, 1991), resulting in different concentration profiles.

166 frames of particle images were acquired at a frequency of 10 Hz using the system shown in Figure 2. Each measurement was conducted four times and the average number of particles per frame was approximately 512. The concentration profile was measured by determining the number of particles for each intensity range and then dividing by the illuminated volume (i.e., the product of the illuminated area and the depth interval). Figure 9 shows the influence of the ionic strength on the near-wall particle concentration profile. The horizontal axis is the depth z and the vertical axis is the concentration of the particles. As expected, the concentration profile of the particles varied depending on the ionic strength of electrolyte. The two profiles have maximums at different depths. The Debye length is estimated using classical DLVO theory and is expressed as

$$1/\kappa = 1\Big/\left\{\left(\sum_i \rho_{i\infty} e^2 z_i{}^2\right)\Big/\varepsilon\varepsilon_0 kT\right\} \tag{4}$$

where e =1.602 x 10^{-19} [C], ε is dielectric constant, ε_0 is the vacuum dielectric constant, k is Boltzmann constant, T is the absolute temperature, and $\rho_{\infty i}$ and z_i are the ionic strength in the bulk and the valence for ionic species i, respectively. The Debye length for both the surface and the fluorescent particles is estimated to be 100 nm for distilled water and it agrees with the result in Figure 9 (repulsive potential for white dots at z < 200 nm). This confirms that an electrolyte solution has a non-uniform concentration distribution for dispersed substances. This result, obtained by direct observation, is an important finding for micro-biochemical analysis, because the presence of a bio-substance in the near-wall region is important for increasing the reaction efficiency and sensitivity. It is thus important to select appropriate ionic characteristics. These surface effects have not been taken into account for conventional micro-biochemical analysis chips. In micro bio-chemical applications, it should be possible to increase the reaction efficiency by accounting for this effect.

In this paper, the concentration profile of nano-particles has been reported. However, this 3D-TIRFM technique can be applied to other applications as well, such as the motion of nano-particles and the reaction efficiency of certain substances.

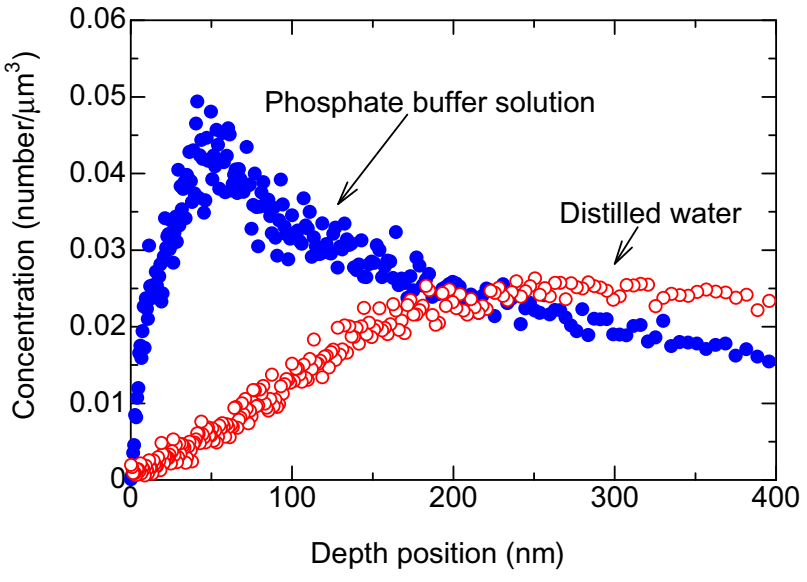

Fig. 9. Concentration profiles of nano-particles near the wall.

4. Particle Realization and Factors in Positional Errors

In this paper, particle realization was carried out for each particle image by assuming that ideal particle images would have a Gaussian profile. The experimentally captured images were image-processed using a Gaussian filter. Cross-correlation between the filtered images and the artificial image gives the particle position in two dimensions. The maximum intensity in the vicinity of the centroid position (3 x 3 pixels) in the original image was taken as the particle intensity. The particle depth was obtained from the particle's intensity, as mentioned above. The uncertainty of particle depth in these measurements is considered below.

(a) Errors Due to Particle Realization

Overlapping of particles and the background intensity level affect particle realization. In this paper, the particle concentration was relatively low (an average of 512 particles per frame). The average size of a particle image was about 14 pixels. This means that the average inter-particle distance is 10 times larger than the average particle image radius.

A high background intensity level (due to a high concentration of particles, out-of-plane particles, and other optical conditions) leads to a miscorrelation between the imaged particles and standard particles. However, the background level due to out-of-plane particles and to optical conditions is negligible when evanescent light is used. In this paper, particle concentration was relatively low and the background intensity level for any condition was zero.

(b) Background Bias

Background bias potentially could affect this measurement. The background bias is due to particle photo-bleaching and occasionally from high particle concentrations. Photo-bleaching become prominent when fluorescent particles are exposed to high light intensities. The exposure time for the particles in evanescent light was approximately 17 s for the concentration measurement, while it was 3 min for particle depth calibration. This can result in a background bias. Photo-bleaching tests performed using a particle attached to a wall surface revealed that the light intensity of the particle decreased to 79 % over 3 min. Thus, photo-bleaching occurred during the 3-min calibration test. However, the exposure time of the particle to intense illumination was short since the particles attached to the pin were moved towards the surface. Note that the illumination intensity is strongest at the wall surface.

(c) Non-Uniform Particle Intensity

The variation in particle size and the aggregation of particles lead to incorrect determination of the particle depth. The fluorescent particles used were well dispersed by using a supersonic washer for 5 min and aggregation is not thought to have occurred. The size fraction of the fluorescent particles was 0.5 % in this paper which is relatively low.

5. Conclusion

A novel 3D-TIRFM technique that was calibrated directly for depth was proposed in this paper. The concentration profile of fluorescent particles in the vicinity of a wall was investigated using this technique. The results showed a non-uniform concentration profile of fluorescent particles near the wall. It is concluded that this is due to the presence of an electrical double layer surrounding the particles and the surface. It is thus important that appropriate electric characteristics should be selected, since non-uniformity and low concentration profiles near walls will affect the reaction efficiency and the sensitivity in micro bio-chemical analysis.

References

Bernard, A., Michel, B. and Delamerche, E., Micromosaic immunoassays, Analytical Chemistry, 73 (2001), 8-12.

Banerjee, A. and Kihm, K. D., Experimental verification of near-wall hindered diffusion for the Brownian motion of nanoparticles using evanescent wave microscopy, Physical Review E, 72 (2005), 042101.
Do, J. and Ahn, C. H., A polymer Lab-On-A-Chip for magnetic immunoassay with on-chip sampling and detection capabilities, Proceedings of μTAS, 1 (2005) 22-24.
Feng, J., Hu. H. H. and Joseph, D. D., Direct simulation of initial valve problems for motion of solid bodies in a Newtonian fluid Part 2 Cuette and Poiseuille flows, Journal of Fluid Mechanics, 277 (1994), 271-301.
Israelachivili, J., Intermomlecular & surface forces (Second edition), (1991), 246-254, Academic Press, London.
Jin, S., Huang, P., Park, J., Yoo, Y. and Breuer, K. S., Near-surface velocimetry using evanescent wave illumination, Experiments in Fluids, 37 (2004), 825-833.
Kihm, K. D., Banerjee, A., Choi, C. K. and Takagi, T., Near-wall hindered Brownian diffusion of nanoparticles examined by three-dimensional ratiometric total internal reflection fluorescence microccopy (3-D R-TIRFM), Experiments in Fluids, 37 (2004), 811-824.
Olsen, M. G. and Adrian, R. J., Brownian motion and correlation in particle imaging velocimetry, Optical Laser Technology, 32 (2000), 621-627.
Sadr, R., Li, H. and Yoda, M., Impact of hindered Brownian diffusion on the accuracy of particle-image velocimetry using evanescent-wave illumination, Experiments in Fluids 38 (2005), 90-98.
Sadr, R., Yoda, M., Zheng, Z. and Conlisk, A. T., An experimental study of electro-osmotic flow in rectangular microchannels, Journal of Fluid Mechanics, 506 (2004), 357-367.
Sato, K., Hibara, A., Tokeshi, M., Hisamoto, H. and Kitamori, T., Microchip-based chemical and biochemical analysis systems, Advanced Drag Delivery Reviews, 55 (2003), 379-391.
Uchiyama, K., Yang, M., Sawazaki, T., Shimizu, H. and Ito, S., Development of a Bio-MEMS for Evaluation of dioxin toxicity by immunoassay method, Sensors and Actuators B, 103 (2004), 200-205.
Zettner, C. M. and Yoda, M., Particle velocity field measurement in a near-wall flow using evanescent wave illumination, Experiments in Fluids, 34 (2003), 115-121.

Author Profile

Kensuke Kanda: He received his M.Sc. (Eng) degree in Mechanical Engineering in 2000 from Tokyo Metropolitan University. He also received his Ph.D. in Mechanical Engineering in 2006 from Tokyo Metropolitan University. He has been working as a researcher at the Advanced Software Technology & Mechatronics Research Institute in Japan since 2006. His research interests are near-wall phenomena, and biological flow and microfluidics.

Satoshi Ogata: He received his M.Sc. (Eng) in Mechanical Engineering in 1997 from Tokyo Metropolitan University, and also received his Ph.D. in Mechanical Engineering in 1999 from Tokyo Metropolitan University. He has been working at the Thermal and Fluid Engineering Division, Tokyo Metropolitan University as a research associate since 1999. His research interests are fluid rheology, microfluidics and drag reduction.

Kazuyoshi Jingu: He graduated from the Precision Engineering Department of Tokyo Metropolitan University in 2006. He is currently a graduate student at the Graduate School of Engineering, Tokyo Metropolitan University.

Ming Yang: He is an Associate Professor of Tokyo Metropolitan University, received his B.Eng., M.Eng. and Dr.Eng. in mechanical engineering from Kyoto University, Japan in 1984, 1986 and 1990, respectively. He worked on intelligent control system for press-brake machine at Research and Development Laboratory of AMADA Co. for one year. From 1991, he moved to Tokyo Metropolitan University and worked on intelligent metal forming system and from 1998 he has been a staff member at the Laboratory of Precision Measurement and Instrumentation and worked on MEMS fabrication and evaluation. He is interested in optimal MEMS design for biological and chemical analysis, micro fluidics of bio-fluid. He is a member of JSME, JSTP, JSPE, JLME and ISCIE.